Int J Clin Exp Med 2019;12(6):6733-6744
www.ijcem.com /ISSN:1940-5901/IJCEM0074085

*Original Article*

# Propofol inhibits burn injury-induced oxidative stress injury through SOD2 up-regulation in human dermal microvascular endothelial cells

Pengwei Shi[1*], Xing Lin[2*], Pengliang Chen[3*], Dequan Xiao[5], Liang Liu[4]

*[1]Emergency Department, [3]The Hui Qiao Medical Centre, [4]Department of Burns, Nan Fang Hospital, Southern Medical University, Guangzhou, P. R. China; [2]Department of Nephrology, People's Hospital of Guizhou Province, Institute of Nephritic and Urinary Disease of Guizhou Province, Guiyang, P. R. China; [5]Department of Breast, Ganzhou Maternal and Child Health Hospital, Jiangxi, P. R. China. [*]Equal contributors.*

Received June 14, 2016; Accepted February 12, 2019; Epub June 15, 2019; Published June 30, 2019

**Abstract:** Burns may induce oxidative stress due to the increased production of reactive oxygen species (ROS) and/or the promotion of cellular oxidation events. The effects of propofol, which plays an important role in antioxidant and organ protection, on burn serum-induced oxidative stress injury and its possible mechanisms were investigated in this study. Burn serum stimulation can lead to cell injuries in human dermal microvascular endothelial cells (HDMECs), including apoptotic cell death and increased cell permeability. Interestingly, these symptoms are alleviated in the presence of propofol. Furthermore, we found that the protective effect of propofol in heat stress-induced cell damage is closely related to its antioxidation. We further revealed that burn serum significantly reduces the level of SOD2 and SOD1 ($P = 0.002$), and propofol was only found to inhibit the reduction of SOD2. The transfection of HDMECs with SOD2 small interfering RNA (siRNA) markedly decreases the expression of SOD2, and the protective effect of propofol in siRNA SOD2 clones is significantly reduced. Taken together, these results indicate that propofol protects the burn serum-injured cells, at least partly through upregulating SOD2 expression to reduce the direct or indirect cell damage caused by oxidative stress.

**Keywords:** Human dermal microvascular endothelial cells, burn serum, oxidative stress, propofol, SOD2

## Introduction

Burns are a common form of traumatic injury and are associated with high mortality and morbidity rates [1]. Blister and edema, resulting from endothelial dysfunction and increased vascular hyperpermeability, are regarded as the classical signs of burn injury [2]. It is well known that burns lead to endothelial dysfunction via vascular damage, the pathogenesis of which includes a complex range of processes such as thermal stimulation, excessive production of reactive oxygen species (ROS), hemodynamic changes and inflammatory mediators [3, 4]. Although adequate fluid resuscitation can improve hypovolemia, it can also markedly aggravate the edema process in the presence of vascular damage. Therefore, reversing vascular damage plays a key role in protecting cells from burn injury.

The ischemic tissue injury that follows thermal injury to the microcirculation in burns has been shown to occur due to increased oxygen demand accompanied by inflammation with coagulopathy [5, 6]. As a potential major mechanism of tissue injury in burns, the excessive production of reactive oxygen species (ROS) has been shown to result in ischemic status via oxidative stress [7]. Accumulating evidence has also implicated that ROS could affect cell signaling in the context of burn injury-induced cellular damage [7, 8]. These previous findings provided a specific mechanism that can be targeted for potential treatment. Manganese superoxide dismutase (SOD2), one of the most important antioxidants, belongs to the superoxide dismutase (SOD) family and is located in the mitochondrial matrix [9]. A high concentration of the enzyme SOD2 in the mitochondria ensures that the basal level of ROS production is neutralized

before it can lead to cell injury [9, 10]. Oxidative stress occurs when this critical balance is disrupted as a result of conditions such as excess ROS production [11], the depletion of antioxidants, or both [12].

Propofol is an i.v. drug that is widely used as a short-acting intravenous anesthetic, and it has been shown to exhibit some antioxidative and anti-inflammatory effects [13]. A previous study demonstrated that propofol prevents oxidative stress-mediated endothelial cell activation and dysfunction induced by hydrogen peroxide, as well as ischemia-reperfusion injury [14]. In this study, we investigated the protective effects of propofol against cellular damage caused by burn serum in HDMECs. We found that the burn serum promoted the oxidative stress response and damage to mitochondria. Furthermore, this burn-dependent injury was inhibited by the up-regulation of SOD2 expression in the presence of propofol.

## Materials and methods

### *Animal model and serum collection*

The experiments were approved by the Animal Care Committee of Southern Medical University (Guangzhou, China) and performed in adherence to the National Institute of Health (USA) guidelines. Burn injuries were inflicted based on a recently described burn model [15]. Briefly, male Sprague-Dawley rats, weighing 160 to 200 g (Laboratory Animal Center of Southern China, China), were anesthetized by peritoneal injection of a mixture of 13.3% ethyl carbamate and 0.5% α-chloralose (0.65 mL/kg). A dorsal area that equaled 25% of the total body surface area was shaved, and the rats were placed in a mold with an adjustable opening to expose the shaved area to a plastic bag holding 90°C to 95°C water for 60 s. This process produced a clearly defined full-thickness burn as confirmed by light microscopy. In the control (non-burn) group, the animals were shaved and subjected to the same procedures except that the temperature of the water in plastic bag was 37°C. Six hours after the burning or sham treatment, blood was collected by cannulation of the carotis communis, and the serum was obtained by centrifugation at 10,000 g for 20 min.

### *Cells and materials*

Human dermal microvascular endothelial cells (HDMECs, ScienCell, USA) were cultured in gelatin-coated plastic culture dishes in a complete MCDB-131 medium supplemented with 10% fetal bovine serum. Propofol was purchased from Sigma-Aldrich (USA), WST-1 was from Clontech Laboratories Inc (Mountain View, CA, USA), MitoSOX™ red mitochondrial superoxide indicator was from Invitrogen (USA). SOD2 and β-actin antibodies were purchased from BD Transduction Laboratories (Lexington, KY, USA) and Sigma-Aldrich (USA), respectively. The 96-well cell culture plates and culture dishes were from Corning (USA).

### *Treatments with burn/normal serum and propofol (PPF)*

The cultured cells were exposed to the serum collected from both the sham treatment and burn groups at 2 h post-treatment. To determine the effect of propofol on the cell damage induced by the burn serum, the cells were pretreated with 1, 10, or 50 mM propofol for 6 h prior to exposure to the sham or burn serum. For selenite treatment, HDMECs were cultured with a serum-free medium supplemented with 20 μM selenite for 6 h under normal conditions. For intralipid treatment, HDMECs were cultured with a serum-free medium supplemented with 10% intralipid (0.2 ml intralipid was added to 1.8 ml serum-free medium) for 6 h under normal conditions.

### *Cell viability assay*

Cell viability was assessed by the Premixed WST-1 Cell Proliferation Reagent (Clontech Laboratories Inc., Mountain View, CA, USA) according to the manufacturer's instructions. Colorimetric changes were determined at 490 nm using a spectrometer to measure viability: the viability at ¼ $OD_{treatment}/OD_{control}$.

### *Transendothelial electrical resistance assay*

Transendothelial electrical resistance (TEER) of HDMEC monolayers was measured with the electrical resistance system (EVOM; World Precision Instruments, Berlin, Germany), as described previously [16]. In brief, HDMECs were seeded on type-IV collagen-coated transwells (0.4 mm pore size; Corning, USA) at a density of $2 \times 10^6/cm^2$. The resistance of the HDMEC monolayer was monitored until stable resistances occurred (> 70 Ω $cm^2$).

*Flow cytometric analysis of cell apoptosis using Annexin V-FITC/PI staining*

Assays were performed according to the manual accompanying the Annexin V-FITC apoptosis detection kit (Invitrogen). Approximately $1 \times 10^6$ cells were collected, washed with ice-cold PBS, and resuspended in a binding buffer containing a suitable amount of Annexin V-FITC. The cells were then incubated at room temperature, in the dark, for 10 min, followed by removal of the buffer by centrifugation. The cells were resuspended in a reaction buffer containing propidium iodide (PI) and flow cytometry analysis was immediately performed to detect the apoptosis.

*Caspase activity by fluorescence spectroscopy*

After treatment with PPF or HS, the cells were harvested and lysates were prepared at -80°C for 30 min, then incubated at 37°C with the caspase substrates: Ac-Asp-Glu-Val-AspAMC (Ac-DEVD-AMC) using a Quadruple Monochromator Microplate Reader (Infinite M1000, Tecan US, NC, USA). The kinetic reaction was monitored for 30 min at 37°C after the addition of the appropriate caspase substrate at a final concentration of 50 μM, using a Spectra Max Gemini spectrofluorimeter (Molecular Devices, Sunnyvale, CA). Caspase-3 activities are represented as relative cumulative fluorescence of the kinetic reaction and compared to those of the untreated controls.

*Measurement of cytosolic cytochrome C*

Cytochrome C ELISA kit (MBL, USA) was used to measure Cytosolic cytochrome C content. The cells were lysed in the cold preparation buffer included in the ELISA kit. Cell homogenates were centrifuged (10,000 g/60 min, at 4°C) and the supernatant was collected. The samples were then treated with a conjugate reagent, and transferred to a cytochrome C antibody-coated microwell plate and incubated for 60 min at room temperature. Next, the plate was washed and treated with a substrate reagent and incubated for 30 min, followed by the addition of stop solution. Finally, the absorbance at 450 nm was detected with an automatic microplate reader (Spectra Max, M5; Molecular Devices, USA). Serial dilutions of a cytochrome C calibrator were assayed along with the samples to establish a standard curve, which was used to calculate the concentration of cytochrome C.

*Mitochondrial superoxide detection*

Mitochondrial superoxide formation was detected by fluorescence microscopy using MitoSOX™ Red as a specific fluorescent probe. Briefly, the cells were incubated with 5 mM of the probe for 30 min at 37°C in the dark. They were then washed thoroughly with warm HBSS buffer and mounted for imaging. Cellular images were captured using a laser scanning confocal microscope.

*Measurement of cellular ATP*

A luciferase-based assay kit (CellTiter-Glo, Promega, USA) was used to measure the intracellular ATP level. Cells were seeded onto a standard 96-well plate, and CellTiter-Glo reagent was added to the wells and allowed to react with a cell lysate for 10 min at room temperature. The luminescence was recorded with an automatic microplate reader (SpectraMax M5; Molecular Devices).

*Mitochondrial membrane potential assay*

The mitochondrial membrane potential was detected using 5,5',6,6'-tetrachloro-1, 1',3,3'-tetraethylbenzimidazolocarbocyanine iodide (JC-1; Molecular Probes, Eugene, OR, USA). Cells were rinsed once with a complete culture medium and incubated with JC-1 for 30 min at 37°C. Then, the cells were centrifuged, washed twice with cold PBS, transferred to a 96-well plate ($10^5$ cells/well), and assayed with a fluorescence plate reader at the following settings: excitation at 490 nm, emission at 540 nm and 590 nm. Changes in the ratio between the measurements of fluorescence intensity collected at test wavelengths of 590 nm (red) and 540 nm (green) are potentially indicative of changes in the mitochondrial membrane.

*siRNA transfection*

Silencer siRNA for SOD2 was designed and synthesized by Guangzhou RiboBio (RiboBioInc, China). The sense sequence was: GGCCUGAUUAUCUAAAAGCtt and the anti-sense was: GCUUUUAGAUAAUCAGGCCtg [17]. Twenty-four hours prior to transfection, HDMECs, at 30-50% confluence, were plated onto a 6-well pla-

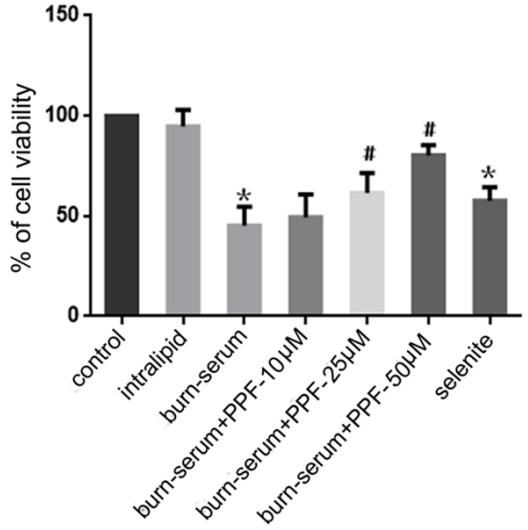


**Figure 1.** Effects of propofol (PPF) or 10% intralipid on HDMEC cell viability after burn serum exposure. HDMECs were treated with various concentrations of PPF (0, 10, 25, 50 μM) followed by burn serum. Cell viability was determined using the WST-1 assay. Selenite at 20 μM was used as a positive control. Each value is the mean ± SD of three determinations. The asterisk indicates a significant difference between the control and test groups, *P < 0.05 as compared with control; #P < 0.05 as compared with burn serum.

te (Nest, Biotech, China), and then transfected using TurboFect™siRNA Transfection Reagent (Fermentas, Vilnius, Lithuania) according to the manufacturer's protocol. The cells were collected after 48-72 hours for further experiments. The mRNA and protein levels of P53 were estimated by RT-PCR and Western blotting.

*Quantitative real-time PCR analysis*

The total RNA isolated from the HDMECs was analyzed for specific transcripts of SOD2 by RT-PCR analysis (upstream primer: 5'-GGAAGCCATCAAACGTGACT-3', downstream primer: 3'-AGCAGGGGGATAAGACCTGT-5'). Total RNA was reverse transcribed with 100 U ReverTra Ace (TOYOBO). The PCR reactions were performed under the following conditions: 94°C for 4 min, specified cycles of 30 s at 95°C, 30 s at 55°C, and 1 min at 72°C. The difference in CT values for the various flow conditions compared to the control was used to determine the relative difference in the level of Mn-SOD mRNA expression.

*Western blotting*

Cell proteins were extracted by using a buffer (20 mM Tris-HCl, 2 mM EDTA, 10 mM EGTA, 0.25 M sucrose, 1:300 protease and phosphatase inhibitor) (Sigma-Aldrich, USA). Samples were centrifuged at 100,000 g for 30 min at 4°C. Then the protein was suspended in an extraction buffer containing 1% Triton X-100. The samples were loaded onto polyacrylamide gels and the membranes were blocked in TBST (20 mM Tris-HCl, 150 mM NaCl, and 0.1% Tween 20) containing 5% nonfat dry milk for 2 h, incubated with the primary antibodies, anti-p53 (Abcam, Cambridge, UK), overnight at 4°C. Peroxidase-conjugated secondary antibody anti-rabbit IgG (Sigma-Aldrich, USA) was used for 90 min. Image J software was used to perform densitometry.

*Statistical analysis*

The experimental data were analyzed for statistical significance using SPSS 13.0 software (SPSS, Chicago, IL, USA). Results were expressed as the mean ± SD of at least three independent experiments. Statistical analysis was performed using a one-way analysis of variance (ANOVA). Statistical significance was determined at $P < 0.05$.

## Results

*Propofol increased cell viability following burn serum exposure*

Cell survival as measured by the WST-1 assay indicated that, as compared with the normal serum group, the burn-serum group exhibited a significantly lower survival rate. The pre-treatment of cells with 10 μM propofol showed no effect on cell survival rate ($P = 0.49$), whereas pre-treatment with 25 μM and 50 μM propofol significantly improved the cell survival rate compared to the burn-serum group ($P = 0.03$, $P = 0.002$, respectively). These results indicated that propofol could protect against burn injury at certain concentrations (**Figure 1**).

*Propofol attenuated burn-serum-induced cell death*

In order to evaluate the effect of propofol on apoptosis caused by burn serum, cells that had undergone pre-treatment with 50 μM propofol followed by burn serum exposure were assessed for apoptosis using quantitative evaluation by flow cytometry. As shown in **Figure 2A**, 50 μM propofol resulted in a marked decrease in burn serum-induced apoptosis in the HDMECs by more than 18% ($P = 0.008$). We also

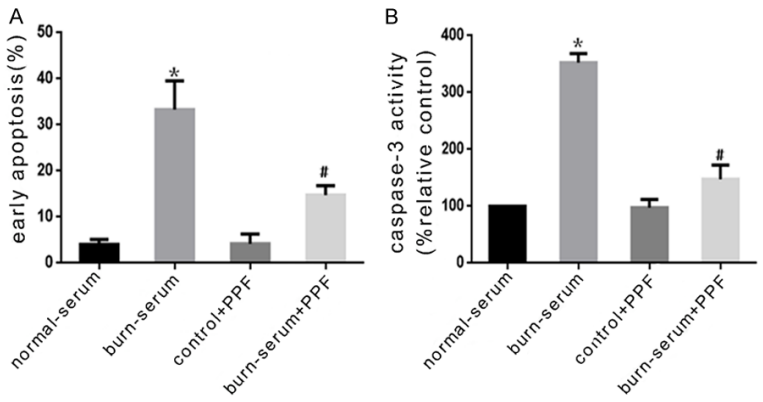


**Figure 2.** Effects of PPF on burn serum-induced apoptosis. A. The apoptotic cells were measured by flow cytometry using Annexin V-FITC/PI staining. B. Enzymatic activity of caspase-3 was tested in cell lysates using the fluorogenic substrate Ac-DEVD-AMC, and the results were expressed as relative to the control at 37°C (100%). Each value is the mean ± SD of three determinations. *P < 0.05 as compared with control; #P < 0.05 as compared with burn serum.

examined the change in activity of effector caspase (caspase-3) and found that propofol significantly reduced capase-3 activity ($P = 0.02$) (**Figure 2B**). These results indicated that propofol exhibits an anti-apoptotic effect in burn serum-treated HUVEC.

*Propofol can protect against burn serum-induced disruption of the HDMEC monolayer*

HDMEC monolayer hyperpermeability was measured by detecting the TEER of cell monolayers. As shown in **Figure 3A**, the exposure of HDMECs to a temperature equivalent of the burn serum for 2 h caused a significant 90% decrease in TEER ($P = 0.001$). Propofol did not alter the permeability of the HDMEC monolayer, but it did protect the TEER from burn serum-induced disruption of the monolayer (**Figure 3A**). Using confocal microscopy, we determined the effect of propofol on the expression of ZO-1 protein. As shown in **Figure 3B**, burn-serum significantly reduced the level of ZO-1 protein, a phenomenon that was inhibited by pre-treatment with 50 μM propofol ($P = 0.005$).

*Propofol inhibited burn serum-induced mitochondria damage*

To demonstrate the effect of propofol on mitochondrial damage induced by burn-serum, we analyzed the changes in mitochondrial membrane potential (⊿Ψm) and the cytosolic cytochrome C level in burn serum-treated HDMECs. The mitochondrial membrane potential (⊿Ψm) was determined by flow cytometry, using the potential-sensitive fluorescent dye JC-1. As shown in **Figure 4A**, compared with the normal-serum group, burn serum stimulation effectively increased mitochondrial membrane potential ($P = 0.02$). However, the effect induced by burn serum was partially inhibited by pre-treatment with 50 mM propofol. As shown in **Figure 4B**, the cytosolic cytochrome C level in the normal serum group was 20.5 ± 5.3 ng/mg protein and reached 83.3 ± 7.7 ng/mg protein in the burn-serum group. The increase of cytosolic cytochrome C induced by burn-serum was significantly reduced to 48.5 ± 5.1 ng/mg protein after pre-treatment with 50 mM propofol ($P = 0.003$). These findings supported the protective role of propofol against mitochondrial damage in burn serum-treated HDMECs. Intracellular ATP levels were also examined to assess mitochondrial dysfunction. As shown in **Figure 4C**, the burn serum led to an obvious decrease in intracellular ATP level, which was reversed by pre-treatment with propofol. This observation indicated that propofol could inhibit burn serum-induced mitochondrial dysfunction.

*Propofol inhibited burn serum-induced mitochondrial superoxide generation*

To examine the antioxidation of propofol, we utilized mitochondria-targeted hydroethidium (MitoSOX™ Red) to investigate mitochondria as the potential source of superoxide generation. As shown in **Figure 5**, burn serum-induced MitoSOX fluorescence intensity significantly differed from the normal serum ($P = 0.04$). Subsequently, we pre-treated cells with 50 μM propofol followed by burn serum exposure. Our results showed that propofol largely suppressed the generation of mitochondrial superoxides induced by burn serum ($P = 0.001$).

*The antioxidation of propofol is involved in the upregulation of SOD2*

SODs, such as SOD1 and SOD2, play a major role in ROS regulation [11]. Therefore, SOD1 and SOD2 levels were monitored after expo-

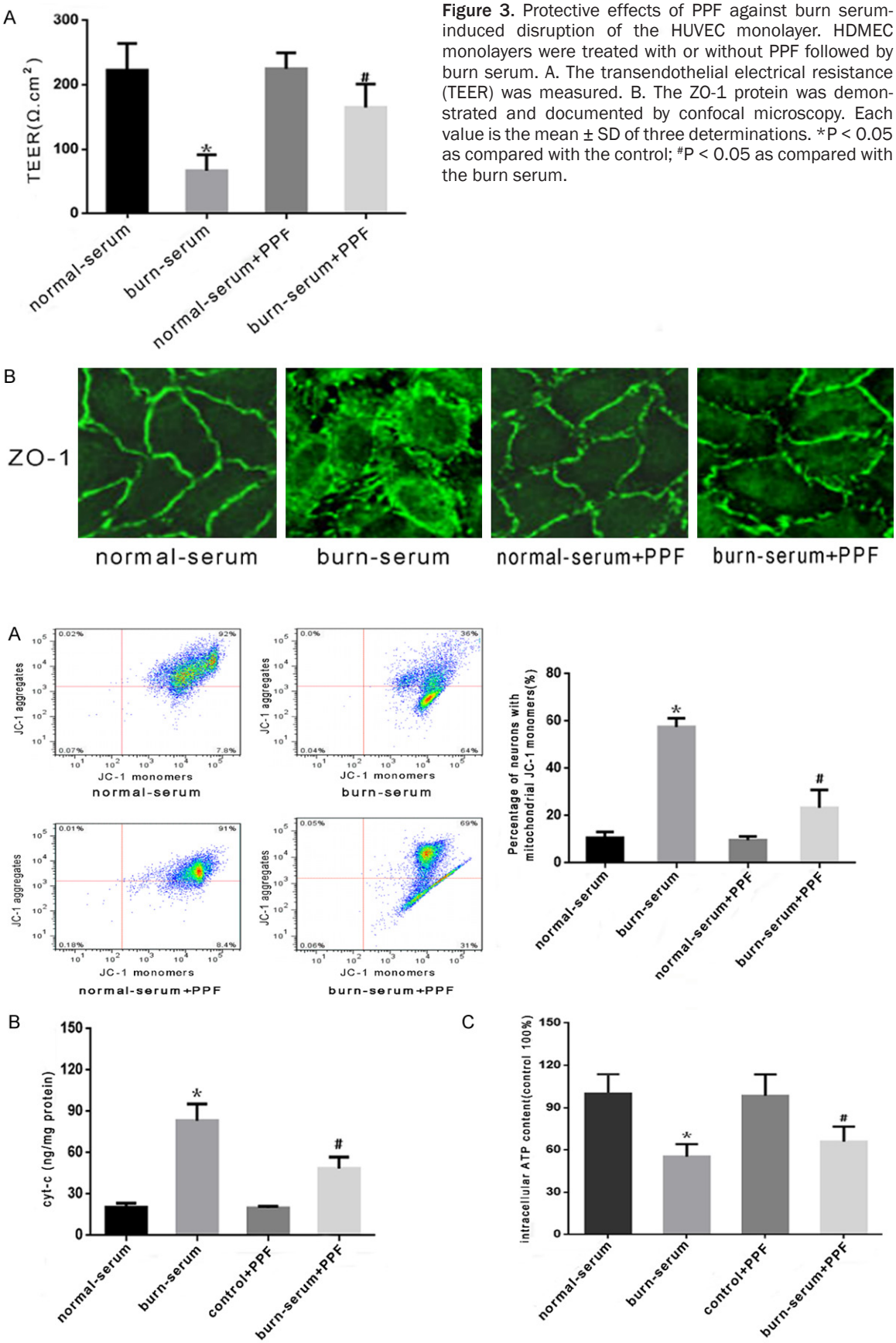


**Figure 3.** Protective effects of PPF against burn serum-induced disruption of the HUVEC monolayer. HDMEC monolayers were treated with or without PPF followed by burn serum. A. The transendothelial electrical resistance (TEER) was measured. B. The ZO-1 protein was demonstrated and documented by confocal microscopy. Each value is the mean ± SD of three determinations. *$P < 0.05$ as compared with the control; #$P < 0.05$ as compared with the burn serum.

**Figure 4.** Burn serum induces mitochondrial damage in HDMECs. A. The loss of ⊿Ψm was measured by JC-1 and analyzed by flow cytometry, and the quantification of the mitochondrial depolarization was expressed as JC-1 monomer (green fluorescence). B. The translocation of cytochrome C from mitochondria into the cytosol was analyzed using a cytochrome C ELISA kit. C. Quantification of the change in the intracellular ATP levels was analyzed using a luciferase-based assay kit. Data are presented as the mean ± SD for three independent experiments, *P < 0.05 as compared with control; #P < 0.05 as compared with burn serum.

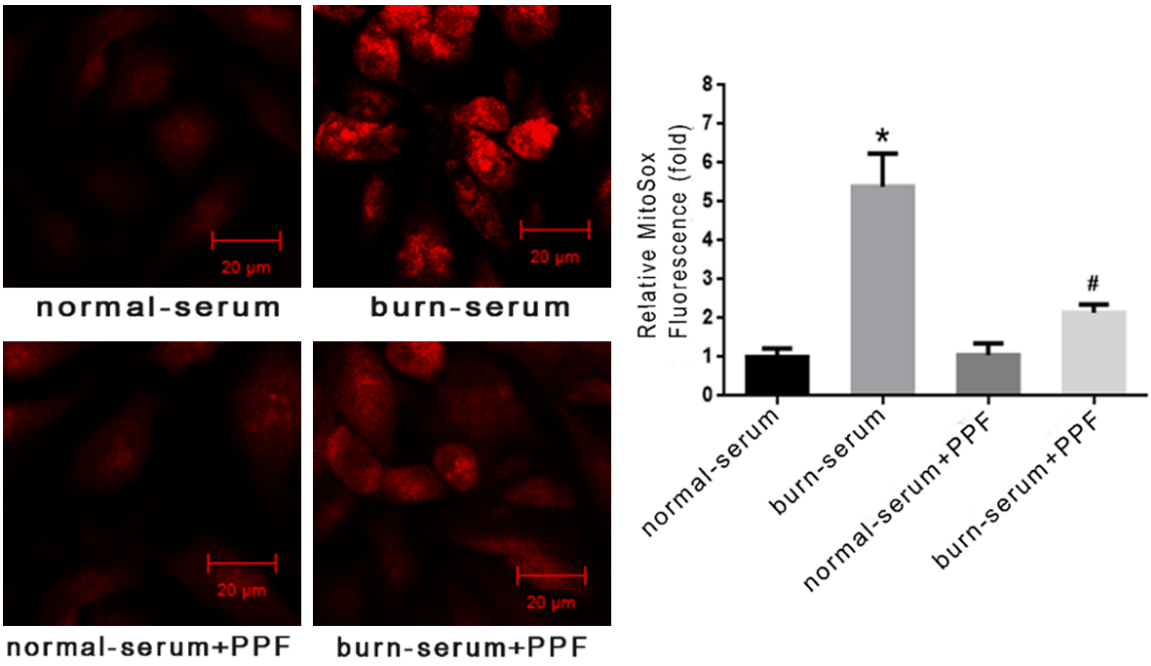


**Figure 5.** Burn serum induces mitochondrial superoxide generation in HDMECs. The HDMECs were treated with or without PPF followed by burn serum and analyzed for mitochondrial superoxide production by fluorescence microscopy using MitoSOX™ Red as a probe. Data are presented as the mean ± SD for three independent experiments, *P < 0.05 as compared with the control; #P < 0.05 as compared with the burn serum.

sure to burn serum with or without propofol pre-treatment. The RT-PCR analysis showed that burn serum significantly reduced mRNA expression of SOD2 and SOD1 compared with the control group ($P$ = 0.002) (**Figure 6A**, **6B**). Although propofol pre-treatment significantly reduced the burn serum-induced inhibition of SOD2 expression ($P$ = 0.03), it did not affect the expression of SOD1 ($P$ = 0.71) (**Figure 6A**, **6B**). Furthermore, the protein levels of SOD1 and SOD2 showed similar results as revealed by Western blot (**Figure 6B**, **6D**). These results suggested that the antioxidation of propofol might be attributed to its effects on the up-regulation of SOD2.

*SOD2 expression was increased in the protective effects of propofol on burn serum-induced cell injury*

To verify the hypothesis that propofol protects against cell damage induced by burn serum through the up-regulation of SOD2 expression, we evaluated the cell injury in the SOD2 knockdown HDMEC clones. The transfected cells were pre-treated with 50 μM propofol followed by a burn serum. Mitochondrial superoxide generation, mitochondria damage (mitochondrial membrane potential, cytosolic cytochrome C level and intracellular ATP level), cells apoptosis and TEER were examined. As shown in **Figure 7A**, MitoSOX fluorescence intensity was significantly increased in the SOD2 siRNA-transfected cells and these cells were more susceptible to burn serum-induced mitochondria damage compared with the scr siRNA-transfected cells (**Figure 7B-D**). Similarly, when compared with scr siRNA cells, SOD2 siRNA-transfected cells showed a drastic decrease in TEER ($P$ = 0.02) (**Figure 7E**) and a significant increase in apoptosis ($P$ = 0.01) (**Figure 7F**). These results indicated that propofol likely inhibits burn serum-induced HDMEC cell injury via the up-regulation of SOD2 expression.

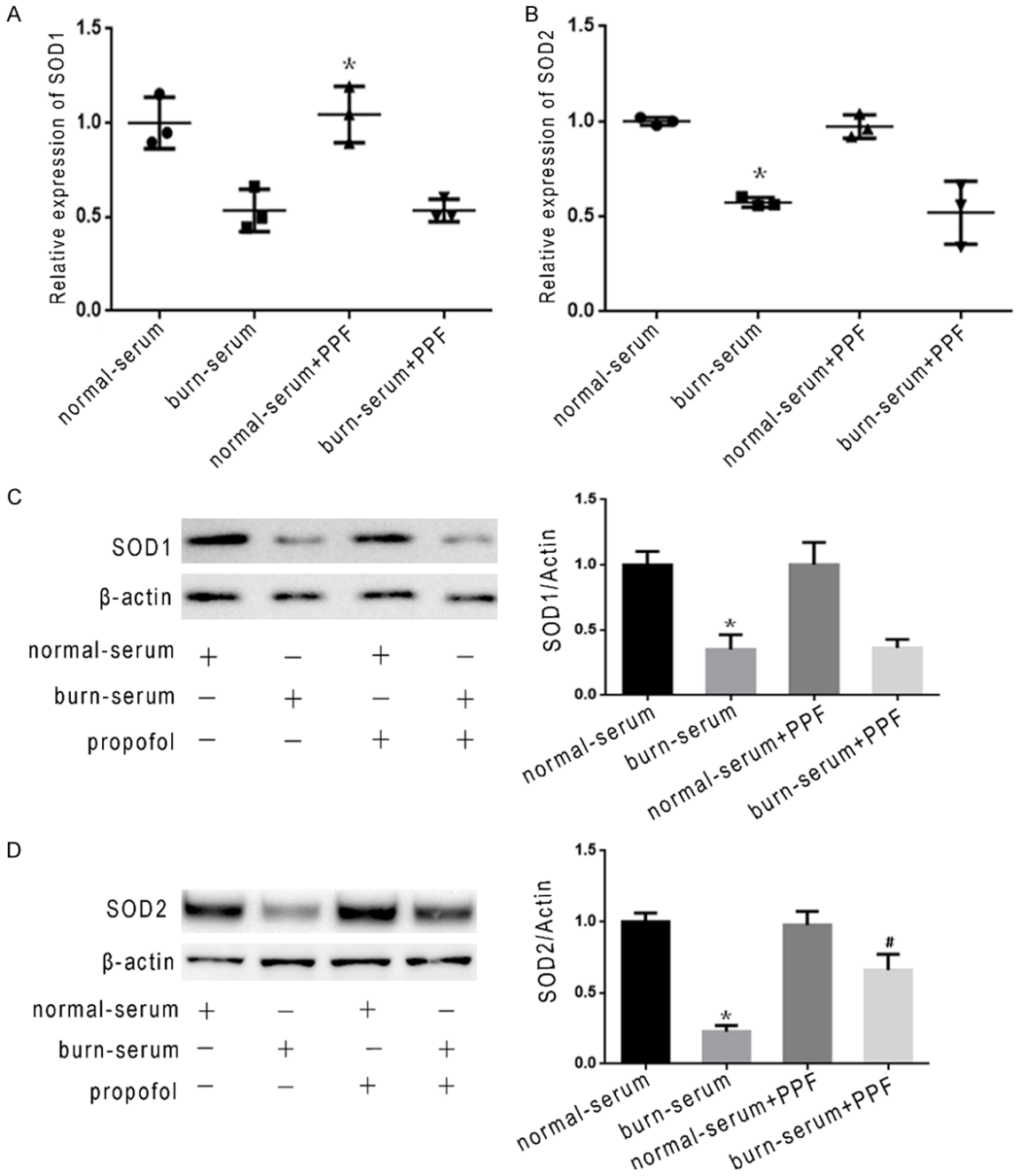


**Figure 6.** The levels of SOD were measured by RT-PCR and western blot assay. A, C. Quantification of the RT-PCR products of SOD1 and SOD2 mRNA. B, D. The protein expressions of SOD1 and SOD2 were assessed by Western blot using β-actin as a loading control. Representative blots from three independent experiments. *P < 0.05 as compared with the control; #P < 0.05 as compared with the burn serum.

## Discussion

In this study, we focused our efforts on understanding the protective effects of propofol against cell death caused by burn serum in HDMECs. In addition, we demonstrated that propofol can attenuate the burn serum-induced disruption of the HDMEC cell monolayer. Moreover, we found that the protective effect of propofol is associated with oxidative stress and the induction of the expression of antioxidant enzyme SOD2.

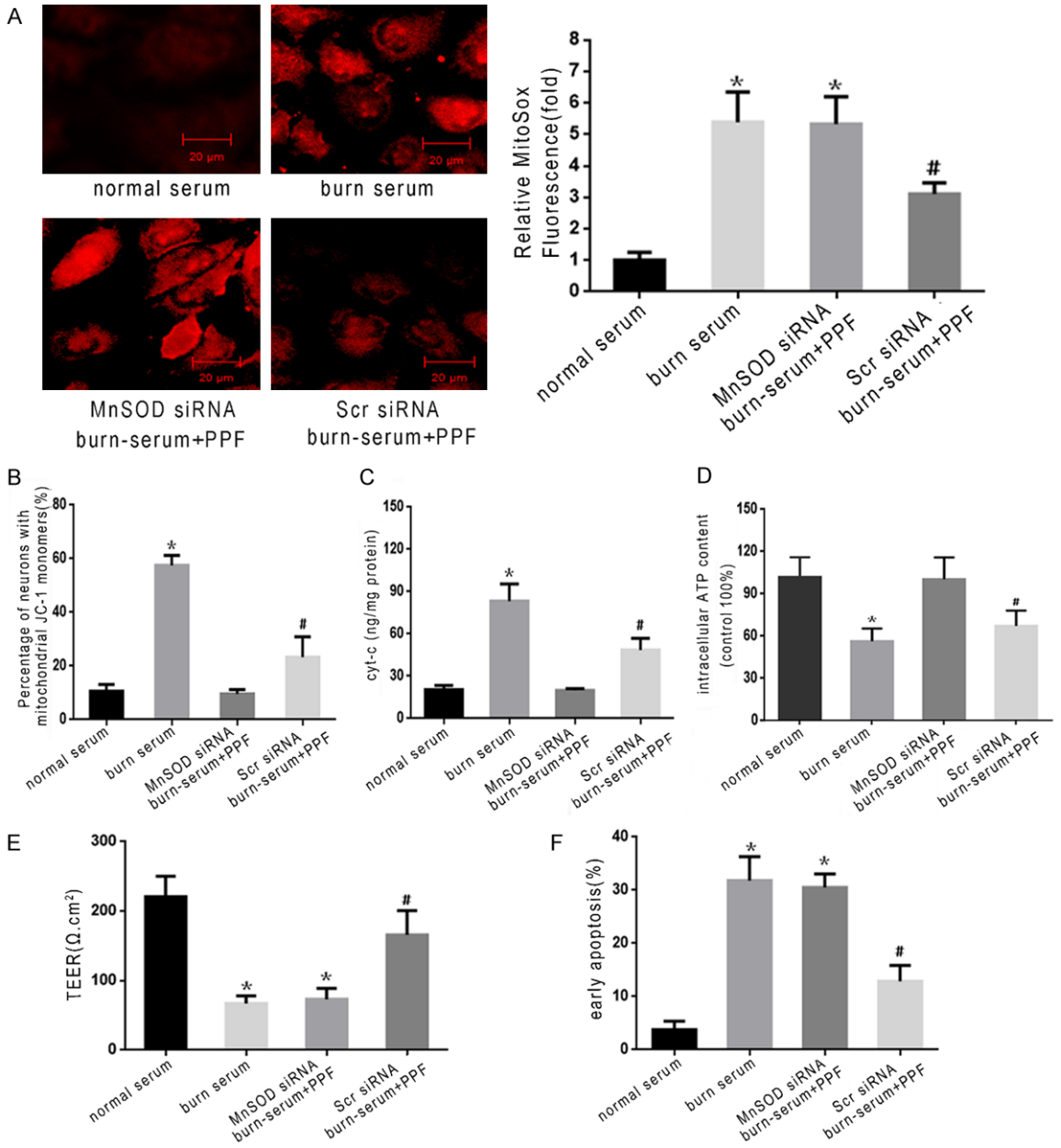


**Figure 7.** The effects of PPF on burn serum-exposed SOD2 siRNA transfected HDMECs. HDMECs were transfected with scrambled siRNA (Scr) or MnSOD siRNA (SOD2). A. The mitochondrial superoxide production was assayed by fluorescence microscopy using MitoSOX™ Red as a probe. B. The loss of ⊿Ψm was measured by JC-1 and analyzed by flow cytometry. C. The translocation of cytochrome C from the mitochondria into the cytosol was analyzed using a cytochrome C ELISA kit. D. Quantification of the change in the intracellular ATP levels was analyzed by a luciferase-based assay kit. E. Disruption of the HUVEC monolayer was evaluated by TEER. F. Apoptotic cells were measured by flow cytometry using Annexin V-FITC/PI staining. Data are presented as the mean ± SD for three independent experiments, #P < 0.05 as compared with the SOD2 siRNA group.

Endothelial cells normally provide an intact monolayer within the lumen of the blood vessel, which functions as a barrier between the bloodstream, its elements and toxins, and tissue parenchyma while also acting as generalized transducing cells that modulate the parenchymal responses to many stimuli [18]. Therefore, the integrity of endothelial cells plays an important role in proper physiological functions. Nevertheless, endothelial cells can be damaged by many factors, such as sepsis [19], burn stress [20], and ischemia reperfu-

sion [21]. Apoptosis has been shown to increase the extent of injuries attributed to burn stress in cell lines and animal models [19, 22, 23]. In addition to apoptosis, the lack of a functioning endothelial cell barrier associated with burn injury is another common symptom in MODS [24]. TEER has been widely used to analyze barrier integrity and the expression of tight junction proteins such as ZO-1 [16]. ZO-1 is important in the establishment and regulation of vascular barrier function as it is correlated with the development of TEER in epithelial cells [25]. Therefore, apoptosis and disruption of the cellular monolayer may co-participate during the pathological process of burn injury. In this study, burn serum-induced cell apoptosis significantly increased in TEER, while it decreased ZO-1 expression. These alterations were partially alleviated by propofol pre-treatment, indicating that propofol inhibited burn serum-induced endothelial cell damage *in vitro*.

To date, several studies have found a link between oxidative stress and burn injury [7, 8, 26], suggesting a synergistic augmentation of cell injury. Mitochondria are the primary source of ROS generation, and are sensitive to oxidative stress injury [27]. Previous reports have illuminated the vital role of ROS in the mitochondrial damage caused by burn stress [28, 29]. In this study, our results confirmed that mitochondrial function was impaired in cells treated with burn serum, as indicated by the release of cytochrome C, an increase in low $\Delta\Psi m$, a decrease in relative ATP content, as well as an increase in MitoSOX fluorescence intensity after burn serum-treatment. These phenomena were restored by propofol, indicating that propofol can inhibit burn serum-induced mitochondrial dysfunction.

As a critical antioxidant enzyme that removes superoxide free radicals, SOD2 is essential in protecting against oxidative damage in cells by buffering mitochondrial ROS production [11]. Loss of SOD2 can give rise to serious events such as aggravated endogenous oxidative stress or cell injury, whereas the up-regulation of SOD2 can prevent injury to cells caused by stress [10, 11]. To investigate the detailed mechanism through which propofol protects mitochondria against the oxidative stress injury induced by burn serum, we studied the effect of propofol on the antioxidant enzymes (Mn SOD and SOD1) in the context of burn serum treatment. Interestingly, propofol could only ameliorate the reduction in SOD2 caused by burn serum in HDMECs, whereas it showed no effect on SOD1 expression. Furthermore, the protective role of propofol against mitochondrial oxidative stress injury was significantly reduced in the SOD2 knockdown cells. Therefore, the protective effect of propofol against burn stress-induced injury can be mainly attributed to anti-oxidation through the up-regulation of SOD2 expression.

In this study, we demonstrated that endothelial damage induced by burn serum can be effectively reversed by propofol treatment. Propofol may act through the oxidative stress signaling pathway and mediate burn-induced cell injury through inhibiting enzyme SOD2 expression. These observations suggest that propofol holds great promise as a potential therapeutic approach in both preclinical and clinical settings as a means of interfering with vascular hyperpermeability caused by burn injury.

## Acknowledgements

This work was supported by the Science and Technology Project of Guangdong Province (no. 2013B060300030) and the Medical Science Foundation of Guangdong Province (no. A20-15015).

## Disclosure of conflict of interest

None.

**Address correspondence to:** Liang Liu, Department of Burns, Nan Fang Hospital, Southern Medical University, No. 1023-1063 Shatai South Road, Baiyun District, Guangzhou 510515, P. R. China. Tel: +86-20-88654523; Fax: +86-20-88654520; E-mail: liuliang9@aliyun.com

## References

[1] Li X, Hammer AM, Rendon JL and Choudhry MA. Intestine immune homeostasis after alcohol and burn injury. Shock 2015; 43: 540-548.

[2] Kahn SA, Bell DE, Stassen NA and Lentz CW. Prevention of hypophosphatemia after burn injury with a protocol for continuous, preemptive repletion. J Burn Care Res 2015; 36: e220-225.

[3] Czapran A, Headdon W, Deane AM, Lange K, Chapman MJ and Heyland DK. International

observational study of nutritional support in mechanically ventilated patients following burn injury. Burns 2015; 41: 510-518.
[4] Ching JA, Shah JL, Doran CJ, Chen H, Payne WG and Smith DJ. The evaluation of physical exam findings in patients assessed for suspected burn inhalation injury. J Burn Care Res 2015; 36: 197-202.
[5] Chen MM, Zahs A, Brown MM, Ramirez L, Turner JR, Choudhry MA and Kovacs EJ. An alteration of the gut-liver axis drives pulmonary inflammation after intoxication and burn injury in mice. Am J Physiol Gastrointest Liver Physiol 2014; 307: G711-718.
[6] Cornick SM, Noronha SA, Noronha SM, Cezillo MV, Ferreira LM and Gragnani A. Toll like receptors gene expression of human keratinocytes cultured of severe burn injury. Acta Cir Bras 2014; 29: 333-338.
[7] Huang YS. Intensive research on the cellular and molecular mechanism of burn shock and ischemic and hypoxic injury. Zhonghua Shao Shang Za Zhi 2005; 21: 324-325.
[8] Zilan A, Cetinkale O, Kiran B, Unlucerci Y, Olgac V, Deniz G and Bekpinar S. The role of supplementation or inhibition of nitric oxide production in burn injury to reduce ischemic damage. Ulus Travma Acil Cerrahi Derg 2003; 9: 169-175.
[9] Winnik S, Gaul DS, Siciliani G, Lohmann C, Pasterk L, Calatayud N, Weber J, Eriksson U, Auwerx J, Van Tits LJ, Luscher TF and Matter CM. Mild endothelial dysfunction in Sirt3 knockout mice fed a high-cholesterol diet: protective role of a novel C/EBP-beta-dependent feedback regulation of SOD2. Basic Res Cardiol 2016; 111: 33.
[10] Miyashita H, Watanabe T, Hayashi H, Suzuki Y, Nakamura T, Ito S, Ono M, Hoshikawa Y, Okada Y, Kondo T and Sato Y. Angiogenesis inhibitor vasohibin-1 enhances stress resistance of endothelial cells via induction of SOD2 and SIRT1. PLoS One 2012; 7: e46459.
[11] Sun G, Wang Y, Hu W and Li C. Effects of manganese superoxide dismutase (SOD2) expression on regulation of esophageal cancer cell growth and apoptosis in vitro and in nude mice. Tumour Biol 2013; 34: 1409-1419.
[12] Qian Z, Liu T, Liu Q, He S, Liu Y, Hou F, Wang X, Mi X, Cai C and Liu X. p53 is involved in shrimp survival via its regulation roles on SOD2 and GPx in response to acute environmental stresses. Comp Biochem Physiol C Toxicol Pharmacol 2014; 159: 38-51.
[13] Bruells CS, Maes K, Rossaint R, Thomas D, Cielen N, Bergs I, Bleilevens C, Weis J and Gayan-Ramirez G. Sedation using propofol induces similar diaphragm dysfunction and atrophy during spontaneous breathing and mechanical ventilation in rats. Anesthesiology 2014; 120: 665-672.
[14] Ozkan D, Akkaya T, Yalcindag A, Hanci T, Gonen E, Gumus H and Delibas N. Propofol sedation in total knee replacement: effects on oxidative stress and ischemia-reperfusion damage. Anaesthesist 2013; 62: 537-542.
[15] Wu W, Huang Q, Miao J, Xiao M, Liu H, Zhao K and Zhao M. MK2 plays an important role for the increased vascular permeability that follows thermal injury. Burns 2013; 39: 923-934.
[16] Lin YL, Chang HC, Chen TL, Chang JH, Chiu WT, Lin JW and Chen RM. Resveratrol protects against oxidized LDL-induced breakage of the blood-brain barrier by lessening disruption of tight junctions and apoptotic insults to mouse cerebrovascular endothelial cells. J Nutr 2010; 140: 2187-2192.
[17] Wu F, Dong XJ, Zhang HQ, Li L, Xu QL, Liu ZF, Gu ZT and Su L. Role of SOD2 in propofol protection of human umbilical vein endothelial cells injured by heat stress. J Anesth 2016; 30: 410-419.
[18] Michiels C. Endothelial cell functions. J Cell Physiol 2003; 196: 430-443.
[19] Gill SE, Rohan M and Mehta S. Role of pulmonary microvascular endothelial cell apoptosis in murine sepsis-induced lung injury in vivo. Respir Res 2015; 16: 1-13.
[20] Wu W, Huang Q, He F, Xiao M, Pang S, Guo X, Brunk UT, Zhao K and Zhao M. Roles of mitogen-activated protein kinases in the modulation of endothelial cell function following thermal injury. Shock 2011; 35: 618-625.
[21] Arfian N, Emoto N, Vignon-zellweger N, Nakayama K, Yagi K and Hirata K. ET-1 deletion from endothelial cells protects the kidney during the extension phase of ischemia/reperfusion injury. Biochem Biophys Res Commun 2012; 425: 443-449.
[22] Wei Z, Wang Y, Luo D, You X, Wang D, Sun G and Wang B. Effect of low-dose cyclophosphamide on the apoptosis of lung parenchyma cells in the early severe burn stage in rats. Zhongguo Xiu Fu Chong Jian Wai Ke Za Zhi 2008; 22: 1429-1432.
[23] Bai X, Fan L, He T, Jia W, Yang L, Zhang J, Liu Y, Shi J, Su L and Hu D. SIRT1 protects rat lung tissue against severe burn-induced remote ALI by attenuating the apoptosis of PMVECs via p38 MAPK signaling. Sci Rep 2015; 5: 10277.
[24] Wang S, Huang Q, Guo J, Guo X, Sun Q, Brunk UT, Han D, Zhao K and Zhao M. Local thermal injury induces general endothelial cell contraction through p38 MAP kinase activation. APMIS 2014; 122: 832-841.
[25] Gardner TW, Lieth E, Khin SA, Barber AJ, Bonsall DJ, Lesher T, Rice K and Brennan WJ. Astrocytes increase barrier properties and ZO-1

expression in retinal vascular endothelial cells. Invest Ophthalmol Vis Sci 1997; 38: 2423-2427.

[26] Klychnikova EV, Tazina EV, Smirnov SV, Spiridonova TG, Zhirkova, EA, Borisov VS and Godkov MA. Correlation between biochemical parameters of oxidative stress, endogenous intoxication and regulation of vascular tone in patients with burn injury. Anesteziol Reanimatol 2015; 60: 45-49.

[27] Luanpitpong S, Chanvorachote P, Nimmannit U, Leonard SS, Stehlik C, Wang L and Rojanasakul Y. Mitochondrial superoxide mediates doxorubicin-induced keratinocyte apoptosis through oxidative modification of ERK and Bcl-2 ubiquitination. Biochem Pharmacol 2012; 83: 1643-1654.

[28] Tzika AA, Mintzopoulos D, Mindrinos M, Zhang J, Rahme LG and Tompkins RG. Microarray analysis suggests that burn injury results in mitochondrial dysfunction in human skeletal muscle. Int J Mol Med 2009; 24: 387-392.

[29] Righi V, Constantinou C, Mintzopoulos D, Khan N, Mupparaju SP, Rahme LG, Swartz HM, Szeto HH, Tompkins RG and Tzika AA. Mitochondria-targeted antioxidant promotes recovery of skeletal muscle mitochondrial function after burn trauma assessed by in vivo 31P nuclear magnetic resonance and electron paramagnetic resonance spectroscopy. FASEB J 2013; 27: 2521-2530.